Journal of the European Ceramic Society **19** (1999) 2173–2181

PII: S0955-2219(99)00027-8
0955-2219/99/$ - see front matter

Microstructure and Mechanical Strength of Diffusion-bonded Silicon Nitride–Molybdenum Joints

A. E. Martinelli* and R. A. L. Drew

McGill University, Department of Metallurgical Engineering, M. H. Wong Building, 3610 University Street, Montreal, QC, Canada, H3A 2B2

(Received 17 August 1998; accepted 12 January 1999)

Abstract

Solid-state bonding of reactive systems, such as Si_3N_4–Mo often results in the formation of excessively thick intermetallic layers that can be detrimental to the final strength of the joint. The objective of this work was to study the microstructural evolution of Si_3N_4–Mo interfaces, aiming at maximum joint strength via a balance between the fraction of bonded material and the amount of interfacial reaction. Joining was carried out under vacuum or nitrogen atmosphere for temperatures between 1100 and 1800°C. Microstructural analyses of the interfaces revealed the presence of Mo_3Si and Mo_5Si_3 along with residual pores. The results from shear strength tests revealed a strong relationship between the microstructure of the interface and the mechanical strength of the joint.

Keywords: intermetallics, joining, interfaces, diffusion, Si_3N_4.

1 Introduction

Silicon nitride features a variety of properties such as resistance to chemically hostile environments, superior mechanical behavior at high-temperatures and low-density.[1–5] However, since it is a brittle material and expensive to fabricate in large complex geometries, small components of this ceramic are usually integrated into larger metallic structures to perform specific tasks. It has been well established[1,6,7] that one of the major challenges in joining ceramics to metals is to overcome the thermo-elastic mismatch between the materials. One alternative to overcome this difficulty is the use of an interlayer, such as a refractory metal, whose linear coefficient of thermal expansion (α) and elastic modulus are similar to that of the ceramic.[8]

Among various options, molybdenum (Mo) can be readily used as an interlayer between Si_3N_4 and most metallic alloys, even if the joint is required to function in corrosive environments. Pure Mo is resistant to high-temperature corrosion by most types of molten glasses and acids found in chemical plants.[9] Nevertheless, the use of Mo as an interlayer implies a new ceramic–metal interface, i.e. between Si_3N_4 and the Mo interlayer. The microstructure and mechanical strength of resulting interface must be studied in order to assess the mechanical reliability of the approach. If a ceramic–metal interface is not characterized by a diffusion or reaction zone, its strength is mainly determined by the work of adhesion and fraction of bonded surface. However, non-reactive and non-diffusive interfaces are limited to just a few ceramic–metal systems, particularly those involving noble metals, e.g. Al_2O_3–Pt.[10] The majority of ceramic–metal combinations, such as Si_3N_4–Mo, result in the formation of either an interfacial diffusion zone or a reaction layer. Thus, it is important to study the mechanism of interface formation and the effect of the growth of reaction layers on the final mechanical strength of the joint.

2 Mo–Si_3N_4 phase equilibria

Figure 1 shows the 1300°C cross-section of the Mo–Si–N phase diagram[11] for the range of partial pressures of N_2 studied herein as the joining environment. The Si_3N_4–Mo interface is also plotted

*To whom correspondence should be addressed at present address: Universidade Federal do Rio Grande do Notre, Department of Physics, Lagoa Nova Campus, Natal, RN, Brazil, 59072-970. E-mail: martinel@dfte.ufrn.br

in the diagram. The Si_3N_4–Mo interface intercepts two tie-lines indicating a sequence of reactions which can be related to the dissociation of Si_3N_4 into elemental Si and $N_{2(gas)}$, and the diffusion of Si into Mo. The corresponding reaction products are the compounds present at the extremities of each tie-line, i.e. Mo_3Si and N_2 for the first reaction, and Mo_5Si_3 and N_2 for the second one. This sequence of reactions indicates that initially Mo_3Si is likely to form by diffusion of Si into Mo. As the phase diagram reflects an equilibrium condition, which is generally not achieved in diffusion-bonded experiments, the transformation from Mo_3Si into Mo_5Si_3 may or may not be observed, depending on the bonding temperature and time. These parameters affect the concentration of diffusing Si at the interface, and therefore, the nature of the resulting silicide. No Mo-nitride is expected to form under the partial pressures of N_2 investigated, suggesting the possible formation of a porous layer at the interface between Si_3N_4 and the reaction zone.

3 Experimental procedure

The starting materials used in this work were Mo-sheet (99·95% pure, Aesar Div., Johnson & Matthey, Toronto), and Si_3N_4 (Ceradyne Inc., Costa Mesa, CA, USA) sintered by the manufacturer using Al_2O_3 and Y_2O_3 as additives. The original plates were cut into small rectangular blocks with cross-section $9{\cdot}0\times9{\cdot}0\,mm^2$ and thickness of the supplied blocks (6·0 mm for Si_3N_4 and 2·5 mm for Mo). The surfaces to be joined were ground, polished (1·0 μm diamond paste finish), and cleaned with isopropanol in an ultrasonic bath for 15 min. The diffusion couples consisted of a block of Si_3N_4 mounted on top of a block of Mo such that their polished surfaces were in contact.

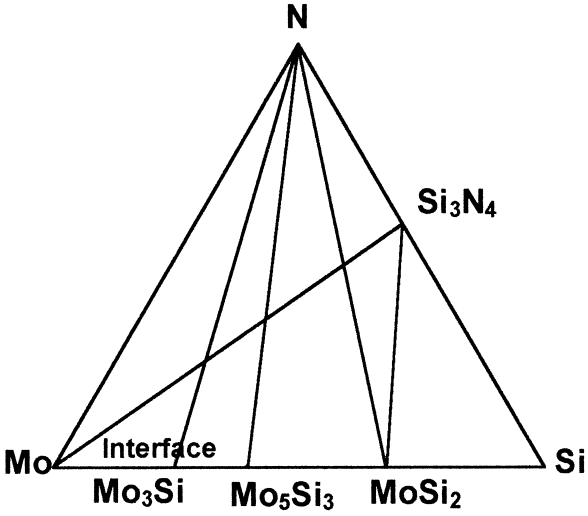

Fig. 1. Isothermal cross-section of the Mo–Si–N phase diagram (1300°C) showing the Si_3N_4–Mo tie-line.

The hot-press equipment consisted of a hydraulic uniaxial press assembled in a graphite resistance furnace [Fig. 2(a)]. The specimens were placed in a graphite die (grade AQ-30, Speer Canada, Montreal) and surrounded by a boron nitride powder-bed (99·5% pure, Aesar Div., Johnson & Matthey, Toronto). The diffusion couples were either annealed under a vacuum of 150 mTorr (20 Pa) or in a N_2 atmosphere. For samples joined under N_2, the furnace was evacuated at room temperature to a pressure of 20 Pa or better and then back filled with gas to pressures slightly above 1 atm (110 to 120 kPa). The furnace was then heated up to the joining temperature at a rate of 15°C min^{-1}. As the furnace temperature reached 10°C below the set point, the load was carefully applied to the sample and monitored by a load cell positioned at the bottom of the furnace. The temperature was measured by an infrared pyrometer inserted at the back of the furnace.

Temperature and pressure profiles are shown in Fig. 2(b). Temperatures ranged from 1100 to 1800°C, the holding time varied from 15 minutes to 4 h, and the uniaxial load was set to 10 MPa. During a joining cycle, the load was maintained within a range of 1 MPa of the nominal value and the temperature within a range of 5°C. After the holding time elapsed, the load was slowly released during

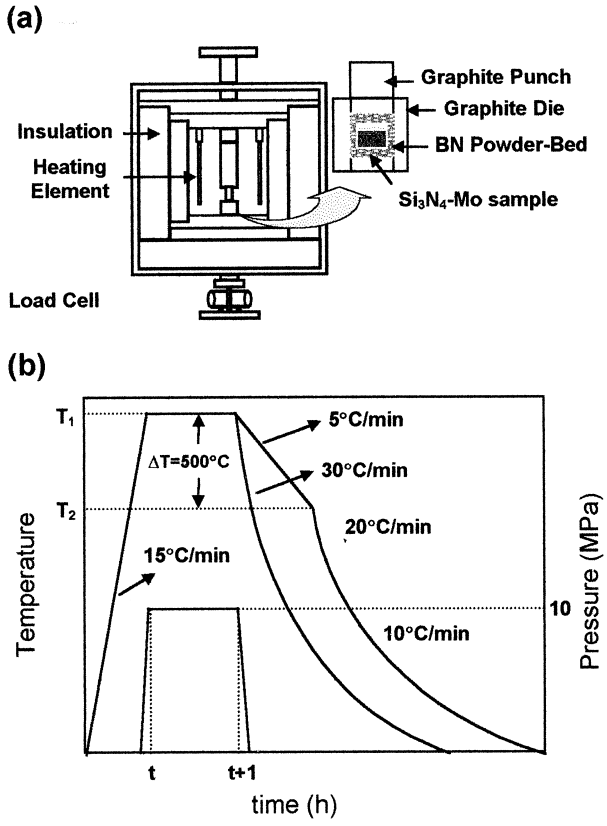

Fig. 2. (a) Schematic representation of the hot-press assembly; (b) temperature and pressure profiles for hot-pressing of Si_3N_4–Mo diffusion couples.

the initial stages of cooling. Two cooling profiles were employed. In the first one, the sample was simply furnace cooled. Average cooling rates for the different stages of this profile are estimated in Fig. 2(b). The second profile consisted of cooling the sample slowly (5°C min^{-1}) for the first 500°C after which the sample was furnace cooled. This profile was used in the preparation of specimens for mechanical testing, as it resulted in a more favourable distribution of residual stresses.[12] Rapid furnace cooling was used to study the kinetics of interface formation. In this case, slow cooling would have resulted in further reaction beyond the stipulated holding time, thus altering the kinetic data. Microstructural characterization of the interfaces was carried out using cross-sections of each joint mounted in cold-setting epoxy resin and cut using a low-speed diamond saw. The specimens were ground and polished with diamond paste, finished with alumina powder (0·05 μm), and cleaned with isopropanol in an ultrasonic bath for 15 min. The thickness of the reaction zones were measured using a Leco 2005 image analyzer. Back-scattered images (BEI) of the interfaces and energy dispersive spectroscopy (EDS) analyses were obtained from a JEOL JSM-840A scanning electron microscope. Electron probe microanalysis (EPMA) of the interfacial phases and X-ray mapping were performed in a JEOL-8900 electron microprobe using wavelength dispersive spectroscopy (WDS). For SEM and EPMA analyses the samples were carbon coated using an Edwards E306A Coating System. X-ray diffraction (XRD) was performed on fracture surfaces of Mo and Si_3N_4 with Cu-K_α radiation using a Rigaku RU-200B diffractometer. The angular range $5 \leq 2\theta \leq 100°$ was scanned at a scan rate of 0·6° min^{-1}. Joint strength was obtained by shearing the joints on an Instron Testing System, Model 8500. Prior to shearing, the samples were surface ground to assure alignment with the plunger. The specimens were then placed in the shear jig with its interface plane parallel to the plane of vertical displacement of the plunger (Fig. 3). The position of the specimen was adjusted so the contact area between the bottom of the plunger and specimen included all its cross-section. The sample assembly was then moved up towards the plunger at a vertical speed of 0·5 mm min^{-1} until the applied load fractured the specimen. Four to six tests were performed for each joining condition.

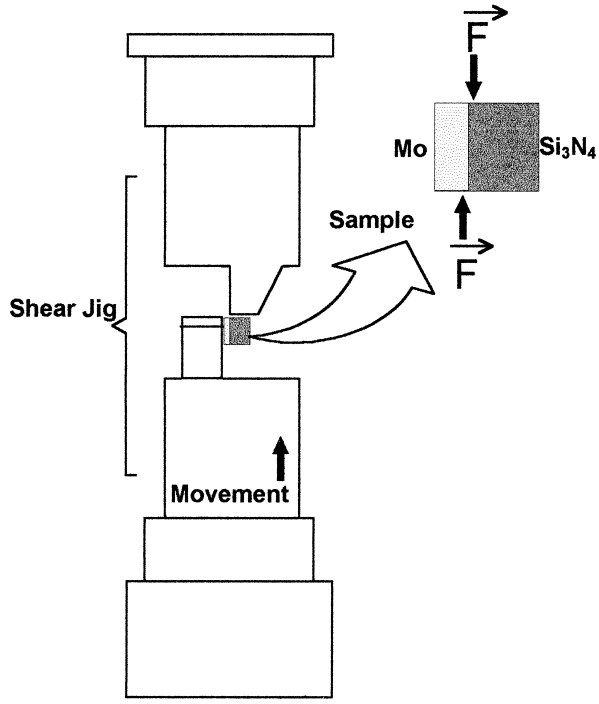

Fig. 3. Schematic representation of shear jig device and assembly.

4 Results and discussion

4.1 Microstructural evolution

Si_3N_4–Mo diffusion couples were hot-pressed at temperatures varying from 1100 to 1800°C, under vacuum and in N_2 atmosphere. Bonding was not observed for samples hot-pressed at temperatures lower than 1200°C, in either vacuum or N_2. At 1100°C, even for the longest holding times (4 h), the fraction of bonded interface was insufficient to establish a reliable joint between the ceramic and metal. As a consequence of limited diffusion, a high concentration of unbonded islands remained at the interface between the Si_3N_4 and Mo, thus preventing joining.

In the range 1200 to 1800°C, Si_3N_4 was successfully joined to Mo under vacuum and in N_2 for bonding times varying from 15 min to 4 h. All samples were hot-pressed with a uniaxial pressure of 10 MPa, as this value is well below the high-temperature compressive yield strength of Mo. Samples prepared both in vacuum and under N_2, between 1200 and 1500°C, developed single-layer interfaces, containing Mo_3Si only.

Plots of the interface thickness as a function of joining time for samples hot-pressed at 1400°C are shown in Fig. 4. The error bars were related to the wavy aspect of the Mo_3Si layers. The interfaces grew in a parabolic fashion. Thus, increasing the holding time from 1 to 4 h did not significantly increase the thickness of the interfaces. Figure 5 shows the interface of a sample joined at 1700°C. The sample was hot-pressed for 1 h under vacuum. Along with Mo_3Si, a porous layer and a BEI contrast could be observed within the interfacial region adjacent to the Si_3N_4. EDS analysis attributed the composition of the new phase to Mo_5Si_3. The formation of this compound occurred by

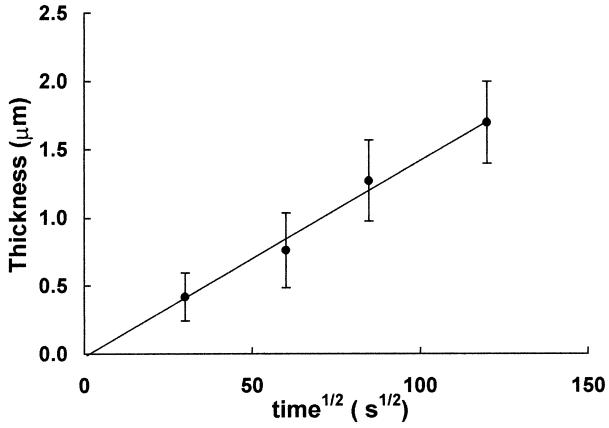

Fig. 4. Thickness of reaction zone as a function of joining time ($T = 1400°C$, under vacuum).

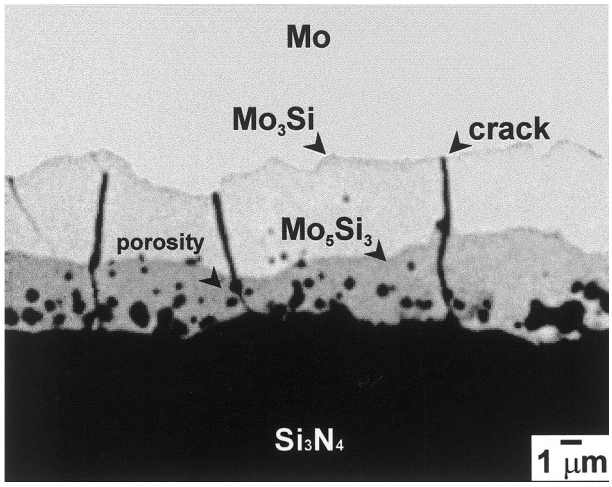

Fig. 5. Electronic image (BEI) of Si_3N_4–Mo interface. Sample hot-pressed under vacuum at $T = 1700°C$, $t = 2$ h, $P = 10$ MPa.

reaction of Si with Mo_3Si, such that:

$$5Mo_3Si + 4Si = 3Mo_5Si_3 \quad (1)$$

Moreover, Si_3N_4 decomposes and reacts with Mo according to the following reaction:

$$Si_3N_4 + 9Mo = 3Mo_3Si_{(s)} + 2N_{2(g)} \quad (2)$$

By heating up Si_3N_4–Mo couples to the joining temperature, $N_{2(g)}$ was produced. When joining experiments were carried out under dynamic vacuum, $N_{2(g)}$ evolved according to eqn (2), was continuously pumped out of the furnace, driving the reaction from left to right. On the other hand, when joining was carried out under N_2 atmosphere, the gas evolved upon the dissociation of Si_3N_4 remained in the environment and would have little effect on the equilibrium of reaction (eqn (1)). Hence the concentration of pores at the interface was related to the evolution of $N_{2(g)}$.

For any particular temperature, Si_3N_4 dissociated more readily under vacuum than in the presence of N_2, resulting in thicker interfaces and also in considerable evolution of N_2. As no reaction is expected to occur between Mo and N_2 under the partial pressures of N_2 investigated, $N_{2(g)}$ resulting from the decomposition of Si_3N_4, could either diffuse into Mo_3Si and Mo, or remain at the interface between the Si_3N_4 and the reaction layer, resulting in porosity. Because of the low solubility of N_2 in both Mo and its silicides, the excess gas remained trapped at the interface forming a porous layer. It has been suggested that, depending on its amount, the N_2 gas could build up significant pressures inside the pores, particularly at relatively high joining temperatures.[11,14] However, this would depend on several factors including how well connected the pores are with the specimen surface. Increasing the joining temperature to 1700°C, increased the total thickness of the interface. Porosity also increased as a result of the extensive dissociation of Si_3N_4. Within the same interfaces, substantial transformation of Mo_3Si into Mo_5Si_3 could be observed.

4.2 Interfacial reaction kinetics

The microstructural evolution of the Si_3N_4–Mo interfaces after joining under vacuum and in N_2, indicated that a similar sequence of events occurred in both cases. However, for joining in N_2, higher temperatures and longer times were required to obtain the same microstructures observed for samples hot-pressed under vacuum. The change in atmosphere from vacuum to N_2 delayed the formation of Mo_3Si, the growth of the porous layer, and the transformation of Mo_3Si into Mo_5Si_3. Nevertheless, changing the environment did not result in different reaction products, nor was the mechanism of diffusion affected. Consequently, the activation energy for interface formation under the different atmospheres remained unchanged. Figure 6 shows an Arrhenius plot of the coefficient of penetration, K_p, as a function of the absolute temperature.

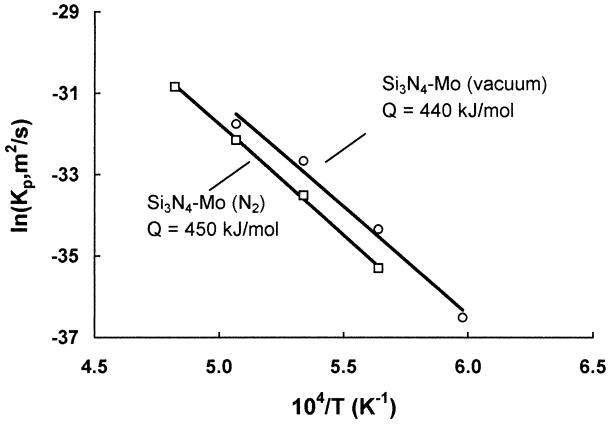

Fig. 6. Arrhenius plot of the coefficient of penetration (K_p) for Si_3N_4–Mo diffusion couples hot-pressed under vacuum and in N_2.

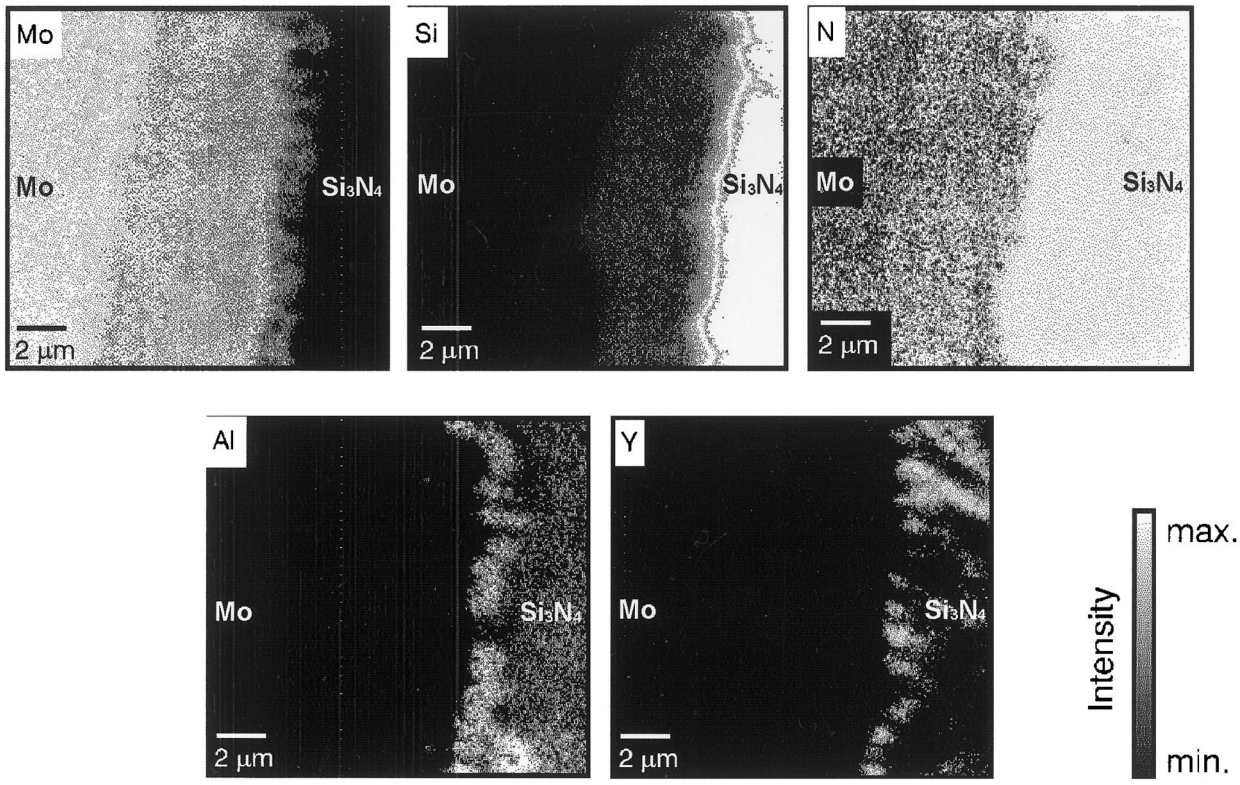

Fig. 7. WDS mapping of atomic species across interface shown in Fig. 5.

$$K_p = K_0 \exp(-Q/RT) \quad (3)$$

The activation energy, Q, for the formation of interfaces was calculated from the slope of the lines obtained under vacuum and N_2. From the Si_3N_4–Mo samples hot-pressed under vacuum, an activation energy of 440 kJ mol^{-1} was obtained. Hot-pressing in N_2 did not result in a significant change of the value of the activation energy (450 kJ mol^{-1}). Although these values were considerably higher than data found in the literature (165 kJ mol^{-1})[4] for samples prepared in a similar manner, they are typical of solid-state diffusion[15,16] and interdiffusion in silicides,[5] which are the likely controlling mechanisms of diffusion-bonding. One difference between the curves for vacuum and N_2 was a slight shift of the frequency factor (pre-exponential term, K_0) to a lower value for the samples hot-pressed in N_2, which accounts for the thinner interfaces compared to the specimens produced under vacuum.

4.3 Electron probe microanalysis

A study of the distribution of atomic species across the Si_3N_4–Mo interface shown in Fig. 5 was carried out by WDS mapping. The main elements analyzed were molybdenum (Mo), silicon (Si), and nitrogen (N). In addition, since Y_2O_3 and Al_2O_3 were used to sinter Si_3N_4, yttrium (Y) and aluminium (Al) contents were also measured. The corresponding maps are shown in Fig. 7, where the interface is aligned in the vertical direction; Mo is at the left side and Si_3N_4 at the right. In the Mo-map, the different contrasts from left to right corresponded to the decrease in the concentration of the element from pure Mo to pure Si_3N_4, passing through Mo_3Si and Mo_5Si_3 areas. No diffusion of Mo into the ceramic was observed, resulting in the dark region characteristic of Si_3N_4. The porous layer could be seen as a dark area indicating that Mo was not present in the region along and beneath the pores. For the Si map, a decrease in intensity, corresponding to a decrease in the concentration of Si, was observed in the direction of Mo, passing through the Mo_5Si_3 and Mo_3Si layers. The porous layer was also seen as a zone depleted in Si as compared to the Si_3N_4 region. Residual Si was observed in the Mo, indicating the presence of traces of dissolved Si, which is consistent with the Mo–Si phase diagram.[17] The concentration of Y and Al increased close to the ceramic interface, clearly delineating the porous layer. However, no diffusion of Al or Y into Mo was observed.

Diffusion profiles across the interface were obtained by WDS line analysis (Fig. 8). Data was collected starting at a distance of about 6 μm inside the Si_3N_4 region ($x = 0\,\mu$m). Until about $x = 5\,\mu$m, the main elements present were Si and N with maximum concentrations 58·9 and 40·3 wt%, which are in good agreement with the nominal composition of Si_3N_4: 60 and 40 wt%, respectively. At $x = 2\,\mu$m, an increase in the Y and O signals

suggested that the probe may have scanned a grain-boundary area containing N-melilite ($Si_3Y_2N_4O_3$). The Al profile indicated the presence of a residual and well distributed concentration of Al (around 1 wt%) across the Si_3N_4 area ($0 \leq \times \leq 4\,\mu m$). The Mo and Si profiles showed good agreement with the data obtained from WDS mapping. The different interfacial phases (Mo_3Si and Mo_5Si_3) could be seen through the variation of the intensities of the WDS signal for these two elements. An increase of the Mo intensity is matched by a decrease in the Si signal indicating the transition from one Mo-silicide to another. For instance, the Si signal reached its maximum at the Si_3N_4–Mo_5Si_3 boundary where the Mo signal reached its minimum. The region corresponding to the pore ($6{\cdot}5 \leq \times \leq 8{\cdot}5\,\mu m$) was characterized by an abrupt increase in the Al, Y, and O intensities, thus confirming the presence of Al and Y deposited within the porous layer, possibly in the form of oxides. The maximum concentrations of Y and Al were respectively 9·3 and 3·4 wt%, which corresponded to typical concentrations of Y_2O_3 and Al_2O_3 used to sinter Si_3N_4. Therefore, although a suspension of Al_2O_3 powder was used to polish the analyzed surface, the observed concentrations of Al were not unusually high, and could not be attributed to residual Al_2O_3 from the polishing procedure. Moreover, pores in the Si_3N_4 region were also analyzed and did not show any spurious increase of the Al signal. As for the O profile, a peak was observed in the same position as the Y-peak, which suggested the presence of a Y–O phase in the area corresponding to the pore. In the same area, the intensity of the N signal showed a slight increase whereas that of Mo decreased, confirming that the porous region contained N but was depleted in Mo. The presence of O

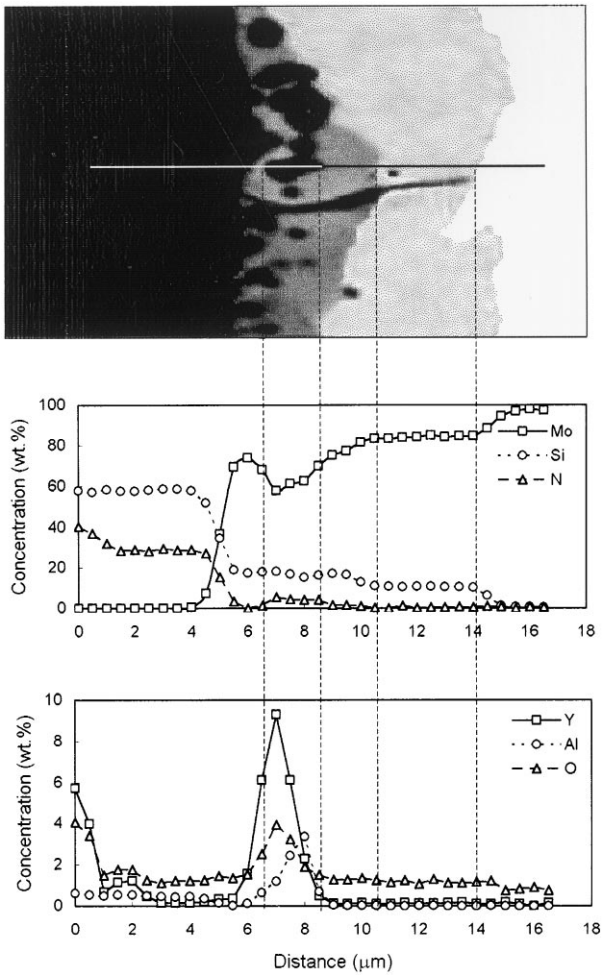

Fig. 8. Quantitative line analysis across interface shown in Fig. 5.

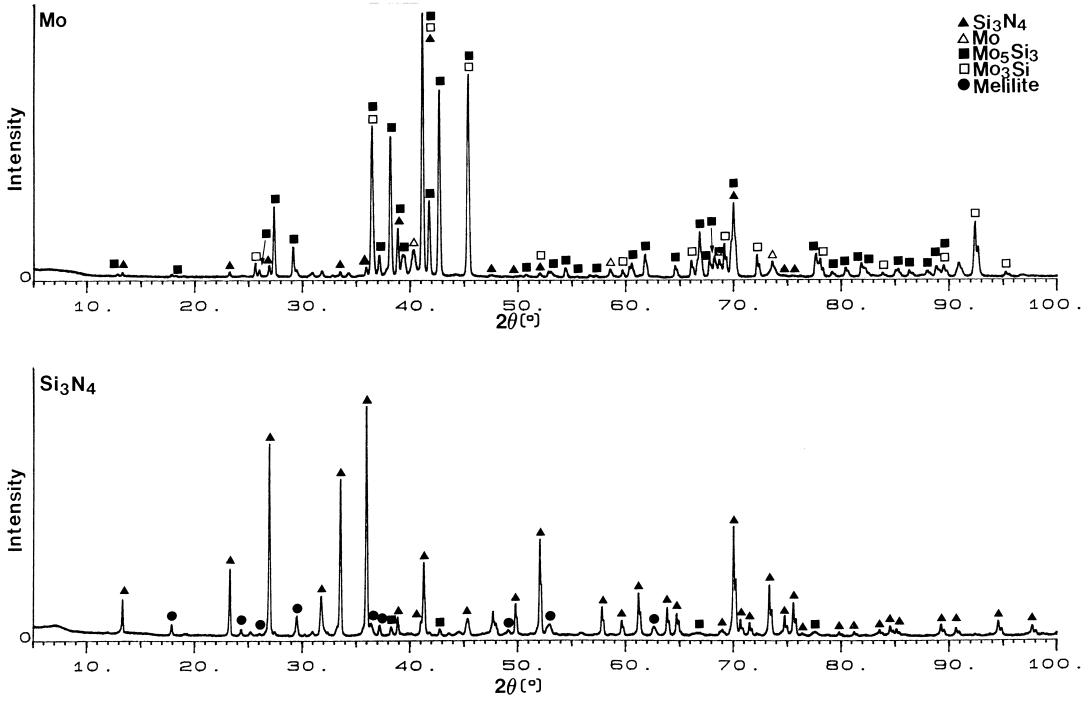

Fig. 9. X-ray diffraction of (a) Mo and (b) Si_3N_4 fracture surfaces for sample hot-pressed at 1700°C for 2 h under N_2.

(4·1 wt% max) in the porous region was established by the existence of a well-defined peak. The same element was not found in the silicide layers and in Mo. A residual intensity of about 1·5 wt% was observed along the entire profile, and could be related to the formation of a surface oxide and/or to background noise. Y and Al were not observed outside the porous layer in the direction of Mo, confirming the corresponding X-ray maps, and indicating that these elements did not diffuse towards the metal.

4.4 X-ray diffraction

X-ray diffraction analyses were performed on fracture surfaces of sheared Si_3N_4–Mo diffusion couples. One of the specimens studied was hot-pressed at 1700°C for 2 h in N_2. The XRD spectra from these surfaces are shown in Fig. 9. Comparing the pattern of the Si_3N_4 fracture surface with that of the original material, it could be seen that upon shearing, most of the interface remained attached to the metal. However, as a consequence of brittle fracture, Si_3N_4 particles remained attached to the Mo fracture surface as well. The main peaks in the Si_3N_4 spectrum corresponded to hexagonal β-Si_3N_4. An intergranular crystalline phase was also observed, consisting in a tetragonal phase of structure similar to that of the mineral melilite ($Ca_2MgSi_2O_7$), and referred to as N-melilite ($Y_2Si_3N_4O_3$). Peaks of Al_2O_3 were not observed, suggesting the presence of an amorphous phase also containing silicon. Comparing these results with the WDS line analysis, within and beneath the porous layer, a mixture of N-melilite and an alumino-silicate or oxynitride glass remained. Low intensity peaks attributed to residual Mo_5Si_3 were also observed. No peaks could be attributed to any Mo-nitride phase, confirming the thermodynamic analysis and WDS results. The X-ray pattern corresponding to the Mo fracture surface revealed the presence of the metal. Residual β-Si_3N_4 was also observed as a result of low-intensity peaks, many of which overlapped with other phases present in greater abundance. The intergranular N-melilite phase was not observed in the Mo fracture surface. The main reaction compounds detected on that spectrum were tetragonal Mo_5Si_3 and cubic Mo_3Si. The concentration of Mo_5Si_3 was slightly higher, confirming the results obtained from BEI and WDS, and was due to substantial transformation of Mo_3Si to Mo_5Si_3 at 1700°C. Furthermore, no Mo-nitrides were identified on the Si_3N_4 fracture surface.

4.5 Shear strength

Joining of Si_3N_4 to Mo was achieved for temperatures as low as 1200°C. The development of residual thermal stresses close to the interfaces did not result in debonding of the joints even for the highest temperature tested (1800°C), which is contrary to previous investigations.[4] Figure 10 shows plots of the shear strength of Si_3N_4–Mo samples as a function of the joining temperature, time, and atmosphere. All samples were slowly cooled at 5°C min^{-1} for the first 500°C, and then furnace cooled to ambient temperature. For samples hot-pressed at 1400°C under vacuum, the average joint strength increased from 30 to 57 MPa, as the bonding time increased from 15 min to 1 h. This improvement was attributed to the initial stages of interface reaction and the formation of a chemical bridge between the two materials. However, as the bonding time increased from 1 to 2 h, and subsequently to 4 h, the average joint strength decreased to 20 and 15 MPa, respectively, as a consequence of the increasing porosity present at the interface. Samples hot-pressed for 1 h under vacuum revealed a similar trend, however, the

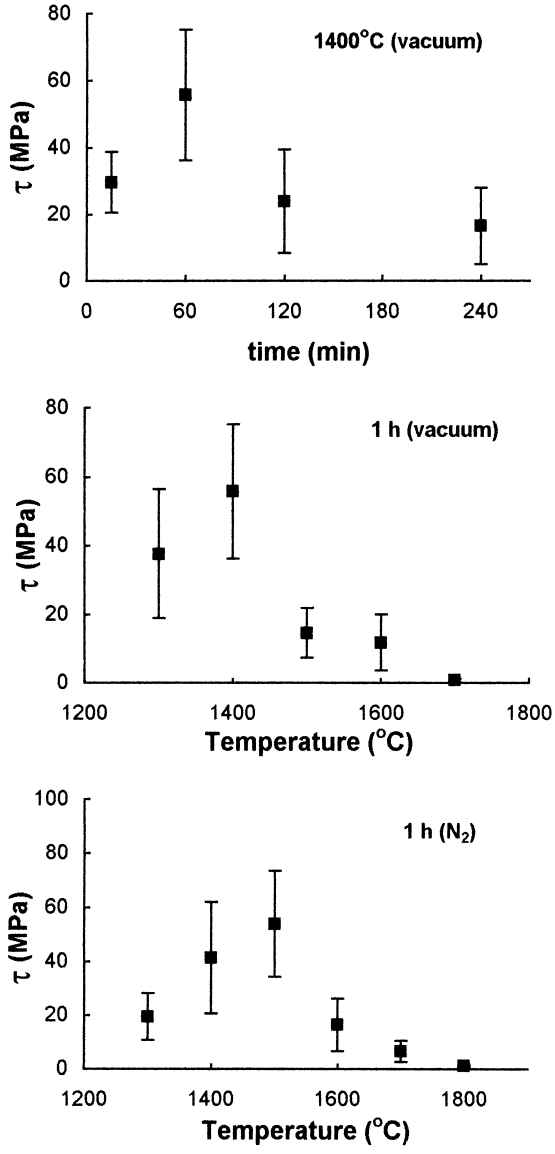

Fig. 10. Shear strength of Si_3N_4–Mo joints as a function of joining time, temperature, and atmosphere.

effect of the temperature was more pronounced than the effect of time. Increasing the joining temperature from 1400 to 1500°C decreased the average joint strength from 57 to less than 20 MPa. The variation in the effect of the temperature and time was clearly related to different growth rates of the reaction zone as a function of these parameters, i.e. exponential versus parabolic.

Strength tests were also performed on joints hot-pressed under N_2 for 1 h. A maximum average strength of 53 MPa was achieved for samples hot-pressed at 1500°C, after which the joint strength decreased as the joining temperature increased. A similar trend was observed when comparing the results obtained from the samples hot-pressed for 1 h under vacuum and in N_2. However, the samples hot-pressed under N_2 achieved their maximum strength at 1500°C, whereas the maximum average strength for the samples hot-pressed under vacuum was attained at 1400°C. The maximum joint strength occurred at about 100°C higher for the samples hot-pressed in N_2, which further confirms that there is a strong relationship between interface microstructure and joint strength. The average joint strength for samples hot-pressed under vacuum at 1400°C and in N_2 at 1500°C, for 1 h, were essentially the same within the error limits for the strength data.

A direct comparison between solid-state bonding and brazing of Si_3N_4 to Mo was obtained. Under optimum conditions (vacuum, 1400°C, 1 h), an average shear strength of 57 MPa was measured for Si_3N_4–Mo diffusion couples. This value represents a significant improvement when compared to shear strength values of the order of 28 MPa reported for Si_3N_4 brazed to Mo at 1300°C using Ni–Cr–Si alloys.[18] Moreover, as a consequence of the nature of the test, shear values are significantly lower than their flexural counterparts. This implies that the actual service strength of the joints produced in this study are potentially higher than the values obtained herein, depending on joint design.

5 Conclusions

1. Molybdenum was joined to Si_3N_4 at temperatures between 1200 and 1800°C. The joining sequence started with the dissociation of Si_3N_4 into Si forming Mo_3Si and further reaction to form Mo_5Si_3.
2. Nitrogen gas evolved, but as a consequence of its limited solubility in the Mo and Mo-silicide layers, the excess gas remained trapped at the interface between Si_3N_4 and Mo-silicides resulting in the formation of a porous layer.
3. Joints produced under vacuum showed thicker interfaces than those prepared in N_2 for similar conditions. Joining in N_2 affected only the kinetics of the process, and therefore, the activation energies for interface formation of interface had similar values for joining in both vacuum and N_2.
4. Although residual thermo-mechanical stresses resulted from the joining process, none of the joints prepared in the temperature range of 1200 to 1800°C debonded upon cooling.
5. Joining was not achieved for temperatures lower than 1200°C implying that the extent of the reaction between Si_3N_4 and Mo was a determining factor in the mechanical reliability of the joints.
6. Shear tests revealed an intimate relationship between the interfacial microstructure and joint strength. The best shear values were obtained for samples hot-pressed under vacuum at 1400°C and in N_2 at 1500°C.

Acknowledgements

The authors acknowledge the Natural Sciences and Engineering Research Council of Canada (NSERC) for partial support of this research and Ceradyne Inc. (Costa Mesa, CA, USA) for supplying the silicon nitride. A.E. Martinelli also thanks CNPq-Brazil for providing his post-graduate scholarship.

References

1. Suganuma, K., Reliability factors in ceramic/metal joining. *Mater. Res. Soc. Symp. Proc.*, 1993, **314**, 51–60.
2. Loh, N. L. and Wu, Y. L., Diffusion bonding of ceramics to metals. *Mater. Manuf. Proc.*, 1993, **8**, 159–181.
3. Sheppard, L. M., Advances in automotive ceramics. *Am. Ceram. Soc. Bull.*, 1990, **69**, 1011–1021.
4. Suganuma, K., Takagi, M., Miyamoto, Y., Koizumi, M., Okamoto, K. and Nakata, H., Joining of silicon nitride to molybdenum under high-pressure. *J. Ceram. Soc. Jpn.*, 1988, **96**, 1051–1056.
5. Shimoo, T. and Okamura, K., Interaction of Si_3N_4 with Cr. *J. Mater. Sci.*, 1994, **29**, 2231–2237.
6. Cawley, J. D., Introduction to ceramic–metal joining. In *Metal–Ceramic Joining*, ed. P. Kumar and V. A. Greenhut. TMS, Chicago, IL, 1991, pp. 3–22.
7. Howe, J. M., Bonding, structure and properties of metal/ceramic interfaces. *Int. Mater. Rev.*, 1993, **38**, 257–271.
8. Baker, H., Benjamin, D., Kirkpatrick, C. W. and Nieman, K. (eds), *Metals Handbook*, 9th edn, ASM International, Materials Park, OH, 1979.
9. Upadhyaya, G. S., Molybdenum and tungsten–their relative assessment. *R and HM*, 1987 168–172.
10. Okamoto, T., Interfacial structures of metal–ceramic joints. *ISIJ Int.*, 1990, **30**, 1033–1034.
11. Heikinheimo, E., Kodentsov, A., Beek, J. A., Klomp, J. T. and Loo, F. J. J., Reactions in the system Mo–Si_3N_4, Ni–Si_3N_4. *Acta Metall. Mater.*, 1992, **40**, S111.
12. Martinelli, A. E., Rogge, R., Fancello, E., Root, J. and Drew, R. A. L., Stress analysis on diffusion bonded SiC–Mo joints. *J. Am. Ceram. Soc*, in press.

13. Schulze, K. K., Jehn, H. A. and Horz, G., High-temperature interactions of refractory metals with gases. *J. Met*., 1988, **40**, 25–31.
14. Lugscheider, E. and Tillmann, W., Methods for brazing ceramics and metal–ceramic joints. *Mater. Manuf. Processes*, 1993, **8**, 219–238.
15. Akselsen, O. M., Diffusion bonding of ceramics. *J. Mater. Sci*., 1992, **27**, 569–579.
16. Kurokawa, K., Interfacial reactions of metals and alloys with Si-based ceramics. *Nippon Kinzoku Gakkai Kaiho*, 1990, **29**, 931–938.
17. Hansen, M., *Constitution of Binary Alloys*. McGraw–Hill, New York, 1958.
18. Hadian, A. M. and Drew, R. A. L., Strength and microstructure of silicon nitride ceramics brazed with nickel–chromium–silicon alloys. *J. Am. Ceram. Soc*., 1996, **79**, 659–665.